Formation and Hydrogen Storage Properties of Dual-Cation (Li, Ca) Borohydride

ARTICLE *in* THE JOURNAL OF PHYSICAL CHEMISTRY C · DECEMBER 2010

Impact Factor: 4.77 · DOI: 10.1021/jp109260g

6 AUTHORS, INCLUDING:

X.D. Kang
Chinese Academy of Sciences
61 PUBLICATIONS **1,456** CITATIONS
SEE PROFILE

Li Hai-Wen
Kyushu University
69 PUBLICATIONS **1,542** CITATIONS
SEE PROFILE

Formation and Hydrogen Storage Properties of Dual-Cation (Li, Ca) Borohydride

Zhan-Zhao Fang,[†] Xiang-Dong Kang,[†] Jun-Hong Luo,[†] Ping Wang,*[,†] Hai-Wen Li,[‡] and Shin-ichi Orimo[‡]

Shenyang National Laboratory for Materials Science, Institute of Metal Research, Chinese Academy of Sciences, Shenyang 110016, China, and Institute for Materials Research, Tohoku University, Sendai 980-8577, Japan

Received: July 5, 2010; Revised Manuscript Received: November 11, 2010

Lithium borohydride, $LiBH_4$, possesses high hydrogen capacity, but cannot be used for hydrogen storage owing to the problematic H-exchange kinetics and thermodynamics. In the present study, we employed the Li^+-Ca^{2+} combination strategy to improve the de/rehydrogenation properties of $LiBH_4$. Our study found that mechanically milling 1:1 $LiBH_4/Ca(BH_4)_2$ mixture formed a dual-cation borohydride, $Li_{0.9}Ca(BH_4)_{2.9}$, which then transformed to stoichiometric $LiCa(BH_4)_3$ in the heating process. The formation and decomposition behaviors of $LiCa(BH_4)_3$ were studied using X-ray diffraction and thermogravimetry/differential scanning calorimetry/mass spectroscopy techniques. It was found that $LiCa(BH_4)_3$ differs significantly from the component phases in terms of physical properties, decomposition behaviors, and mechanistic pathway. In particular, $LiCa(BH_4)_3$ exhibits improved de/rehydrogenation properties relative to the component phases. These experimental findings exemplified the effectiveness of manipulation of dual-cation combination in tuning the de/rehydrogenation properties of the ionic light-metal borohydrides.

1. Introduction

Lack of safe and efficient means for on-board hydrogen storage is a major obstacle to the widespread use of hydrogen as an energy carrier, particularly for vehicular applications.[1,2] Recently, light-metal borohydrides, e.g., $LiBH_4$, $Mg(BH_4)_2$, and $Ca(BH_4)_2$, have attracted considerable interest as potential high-capacity hydrogen storage media.[3−16] The past decade has witnessed significant progress in addressing the kinetic and thermodynamic limitations of the ionic borohydrides that are essentially imposed by the strong chemical bonds. For example, reactant destabilization,[17−23] tailoring nanophase structure by using foreign scaffolds,[24−27] cation/anion substitution,[8,28] and catalyst doping[29−32] are all proven effective means for improving the reversible dehydrogenation properties of $LiBH_4$. However, even with the aid of these technological advances, the hydrogen storage properties of ionic borohydrides and related materials are still far below those required for practical on-board applications. This necessitates the further exploration of novel composition/structural tailoring technologies.

The coupled experimental/theoretical studies of Orimo et al. found that the thermodynamic stability of the ionic borohydrides can be correlated fairly well with the Pauling electronegativity of the metal cations.[33,34] This finding suggests that manipulation of multication combination may provide a general route for tuning the thermodynamic stability of borohydrides. Employment of this strategy has yielded several novel dual-cation borohydrides.[35−44] Li et al. prepared $ZrLi(BH_4)_5$ and $ZrLi_2(BH_4)_6$ by mechanically milling $LiBH_4/ZrCl_4$ mixtures in appropriate molar ratios, and they observed a dehydrogenation temperature decrease of the dual-cation (Li, Zr) borohydrides relative to $LiBH_4$.[35] By calcining the prehomogenized $LiBH_4/KBH_4$ mixture at moderate temperature, Nickels et al. successfully prepared mixed alkali metal borohydride, $LiK(BH_4)_2$, which exhibits an intermediate decomposition temperature between those of the constituent phases.[36] Quite recently, Lee et al. reported a systematic study of the $xLiBH_4 + (1 - x)\alpha$-$Ca(BH_4)_2$ composite system (x ranges from 0 to 1).[45] Their study found that the postmilled samples are physical mixtures of the constituent phases, which undergo a eutectic melting over a wide composition range. In our recent study of the ionic borohydrides, we focused on the preparation and characterization of mixed alkali and alkaline-earth metal borohydrides, aiming at developing novel dual-cation borohydrides with favorable combination of high hydrogen capacity, moderate thermodynamic stability, and fast hydrogen exchange kinetics. In our study of the $LiBH_4/Ca(BH_4)_2$ system, we got significantly different experimental findings from those of Lee et al. Our study found that mechanically milling 1:1 $LiBH_4/\beta$-$Ca(BH_4)_2$ mixture generated a new dual-cation (Li, Ca) borohydride, $Li_{0.9}Ca(BH_4)_{2.9}$, which further transformed to $LiCa(BH_4)_3$ at elevated temperatures. In comparison with the component phases, $LiCa(BH_4)_3$ exhibited improved dehydrogenation properties and different decomposition pathways. These experimental findings may serve as a fundamental basis for developing high-performance borohydrides for reversible hydrogen storage.

2. Experimental Section

The starting materials, $LiBH_4$ (≥90% purity) and $Ca(BH_4)_2 \cdot 2THF$ powders, were purchased from Sigma-Aldrich Corp. $LiBH_4$ was used as received. The adduct-free $Ca(BH_4)_2$ was prepared by heating $Ca(BH_4)_2 \cdot 2THF$ under dynamic vacuum at 200 °C for 10 h. The $LiBH_4/Ca(BH_4)_2$ mixture in a 1:1 molar ratio was mechanically milled under Ar (99.999% purity) atmosphere for 10 h by using a Fritsch 7 planetary mill at 400 rpm in a stainless steel vial together with eight steel balls (10 mm in diameter). The ball-to-powder ratio was around 40:1. For comparison, the individual $LiBH_4$ and $Ca(BH_4)_2$ samples were also milled under identical conditions. All sample han-

* To whom correspondence should be addressed. Fax: +86 24 2389 1320. E-mail: pingwang@imr.ac.cn.
[†] Chinese Academy of Sciences.
[‡] Tohoku University.

10.1021/jp109260g
Published on Web 12/06/2010

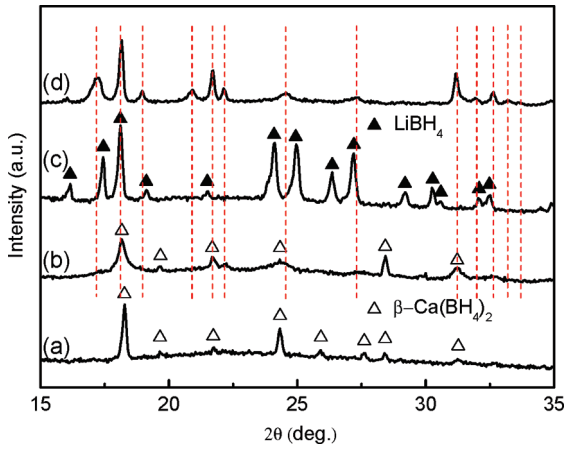

Figure 1. XRD patterns of (a) as-prepared adduct-free $Ca(BH_4)_2$, (b) postmilled $Ca(BH_4)_2$, (c) postmilled $LiBH_4$, and (d) postmilled $LiBH_4$/$Ca(BH_4)_2$.

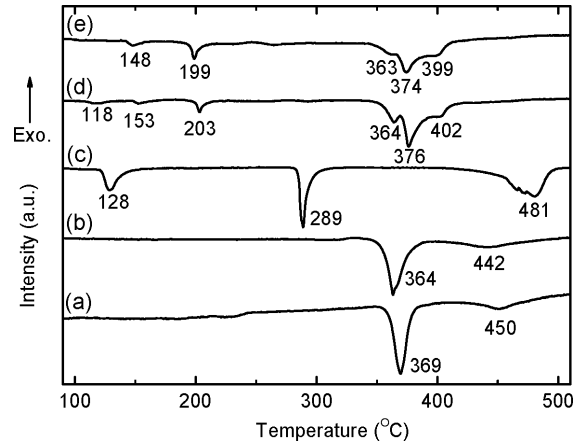

Figure 2. DSC profiles of (a) as-prepared adduct-free $Ca(BH_4)_2$, (b) postmilled $Ca(BH_4)_2$, (c) postmilled $LiBH_4$, (d) postmilled $LiBH_4$/$Ca(BH_4)_2$, and (e) posttreated $LiBH_4/Ca(BH_4)_2$ at 210 °C.

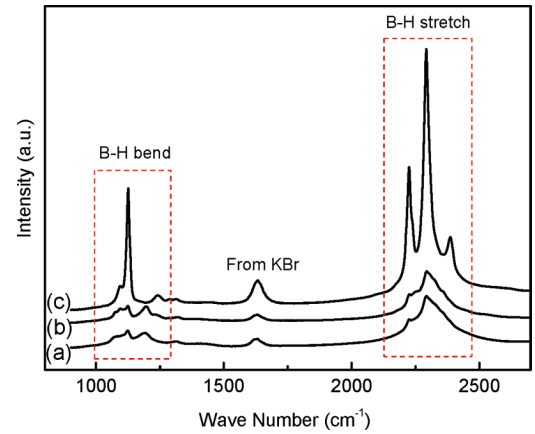

Figure 3. FTIR patterns of the postmilled samples: (a) $Ca(BH_4)_2$, (b) $LiBH_4/Ca(BH_4)_2$, and (c) $LiBH_4$.

dlings were performed in an Ar-filled glovebox, which was equipped with a circulative purification system to maintain the H_2O and O_2 levels typically below 0.1 ppm.

The physical and chemical transformations of the postmilled $LiBH_4/Ca(BH_4)_2$ and related samples were examined by using synchronous thermogravimetry/differential scanning calorimetry/mass spectroscopy (TG/DSC/MS; Netzsch 449C Jupiter/QMS 403C). In the thermal analyses, the sample was heated at a ramping rate of 5 °C/min under a flowing Ar (99.999% purity) atmosphere. The dehydrogenation/rehydrogenation properties of the samples were examined using a carefully calibrated Sievert type apparatus. In a typical dehydrogenation measurement run, the reactor containing the sample with an amount of around 100 mg was first evacuated to a pressure less than 100 Pa, and then heated to 450 °C, followed by holding at this temperature for 2 h. The subsequent rehydrogenation of the decomposed sample was carried out at 400 °C under an initial hydrogen pressure of 10 MPa for 12 h. To minimize H_2O/O_2 contamination, the high-purity hydrogen (99.999%) was further purified using a hydrogen storage alloy system.

The samples were characterized by powder X-ray diffraction (XRD; Rigaku D/MAX-2500, Cu Kα radiation) and Fourier transform infrared spectroscopy (FTIR; Bruker TENSOR 27, DLaTGS detector, 4 cm^{-1} resolution). All the samples for XRD or FTIR analyses were prepared in the Ar-filled glovebox. To minimize the H_2O/O_2 contamination during the XRD measurement, a thin layer of grease was smeared on the surface of the samples. FTIR analysis was carried out using the KBr-pellet method, and the obtained spectra were normalized using OPUS 6.5 software.

3. Results and Discussion

3.1. Formation of Dual-Cation Borohydride $LiCa(BH_4)_3$. Mechanically milling the 1:1 $LiBH_4/Ca(BH_4)_2$ powder mixture results in the formation of a new dual-cation (Li, Ca) borohydride. This was evidenced by the combined XRD, DSC, and FTIR analyses. As shown in Figure 1, XRD examination of the postmilled $LiBH_4/Ca(BH_4)_2$ sample could hardly detect the starting materials, but did detect a new set of diffraction peaks that cannot be indexed to any known phase(s). Here, it should be noted that several strong peaks of the postmilled $LiBH_4$/$Ca(BH_4)_2$ sample are close to those of $LiBH_4$ or $Ca(BH_4)_2$ (e.g., the peaks at $2\theta = 18.2°$, 21.7°, and 31.2°). However, a careful examination of the whole diffraction patterns found that this was just a coincidence, as many other diffraction peaks of $LiBH_4$ and $Ca(BH_4)_2$ were very weak or even undetectable in the postmilled sample. In line with the XRD result, DSC analysis of the postmilled $LiBH_4/Ca(BH_4)_2$ sample detected very weak endothermic peak at ~118 °C that corresponds to the polymorphic transformation of the residual $LiBH_4$, as shown in Figure 2. Assuming that other species exert no influence on the polymorphic transformation of $LiBH_4$, the residual $LiBH_4$ amount in the postmilled sample was estimated to be around 10% on the basis of the quantitative analysis of the phase transition enthalpies of the milled $LiBH_4/Ca(BH_4)_2$ and neat $LiBH_4$ samples. The residual $LiBH_4$ in the postmilled sample should be completely consumed in the subsequent heating process since the endothermic peak at ~289 °C that corresponds to the melting reaction of $LiBH_4$ was not detected in the DSC analysis, as seen in Figure 2. A close examination further found that the XRD pattern of the postmilled $LiBH_4/Ca(BH_4)_2$ sample resembles that of the starting material β-$Ca(BH_4)_2$, indicating that the newly formed phase may possess a crystal structure similar to that of β-$Ca(BH_4)_2$. This was further supported by the parallel FTIR analysis. As shown in Figure 3, the IR spectrum of the milled $LiBH_4/Ca(BH_4)_2$ sample resembles that of milled $Ca(BH_4)_2$, but differs significantly from that of $LiBH_4$ in terms of the characteristic B−H bands. These findings, together with the fact that no appreciable gas desorption occurs in the milling process, suggest that the majority of $LiBH_4$ most likely dissolves into the parent β-$Ca(BH_4)_2$ lattice during the mechanical milling process, producing a new dual-cation borohydride with a composition close to $Li_{0.9}Ca(BH_4)_{2.9}$, which

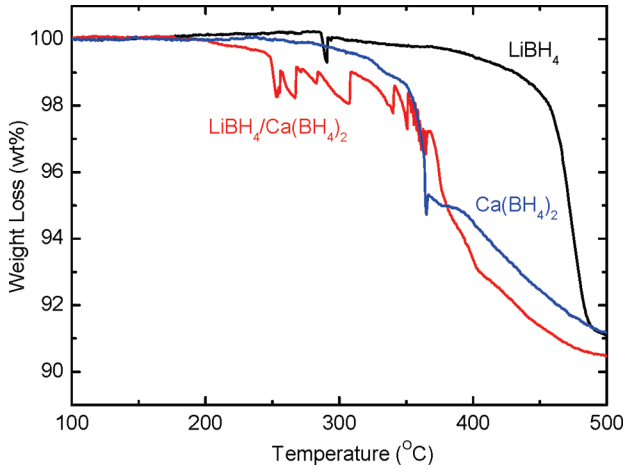

Figure 4. TG profiles of postmilled $LiBH_4$, $Ca(BH_4)_2$, and $LiBH_4/Ca(BH_4)_2$ samples.

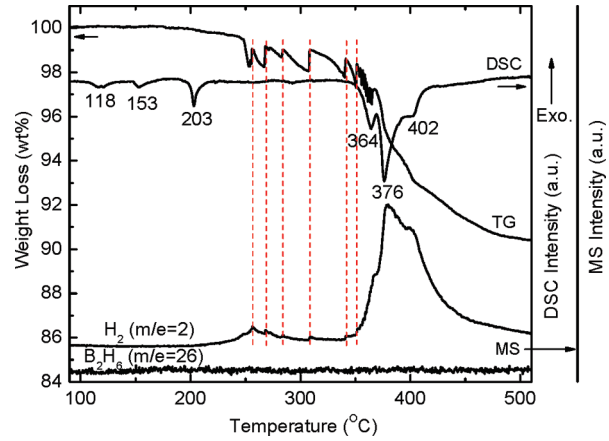

Figure 5. Synchronous TG/DSC/MS profiles of postmilled $LiBH_4/Ca(BH_4)_2$ sample.

then transforms to stoichiometric $LiCa(BH_4)_3$ during the heating process following eq 1. This was further supported by comparison of the DSC profiles of the postmilled and postheated $LiBH_4/Ca(BH_4)_2$ samples at 210 °C. As seen in Figure 2e, the weak endothermic peak at ~118 °C that corresponds to the polymorphic transformation of the residual $LiBH_4$ disappeared after heat treatment at 210 °C. Additionally, the posttreated sample exhibits lower phase transformation temperature and melting point (as discussed below) compared to the postmilled sample, which should be associated with the composition change arising upon incorporation of the residual $LiBH_4$ into the dual-cation borohydride. Judging from the applied preparation conditions, the solid phase reaction between $LiBH_4$ and β-$Ca(BH_4)_2$ should be a thermodynamically and kinetically favorable process.

$$LiBH_4 + Ca(BH_4)_2 \xrightarrow{\text{milling}} Li_{0.9}Ca(BH_4)_{2.9} + 0.1LiBH_4 \xrightarrow{\text{heating}} LiCa(BH_4)_3 \quad (1)$$

3.2. Study of Decomposition Behaviors of $LiCa(BH_4)_3$. Property examination found that $LiCa(BH_4)_3$ exhibited distinct decomposition behaviors from the constituent phases. Figure 4 presents the TG profiles of the postmilled $LiBH_4$, $Ca(BH_4)_2$, and $LiBH_4/Ca(BH_4)_2$ samples. The decomposition behaviors of the individually milled $LiBH_4$ and $Ca(BH_4)_2$ were found to agree well with the literature results.[13,32,46] However, after being milled together, the characteristic decomposition behaviors of $LiBH_4$ and $Ca(BH_4)_2$ were no longer detectable. The newly formed $LiCa(BH_4)_3$ was observed to decompose from ca. 200 °C, much lower than the onset decomposition temperatures of the component phases (ca. 400 °C for $LiBH_4$ and ca. 300 °C for $Ca(BH_4)_2$). After being heated to 500 °C, $LiCa(BH_4)_3$ showed larger weight loss than the component phases (9.6 vs 8.8 wt %). Additionally, $LiCa(BH_4)_3$ exhibited acute weight fluctuations that distinguish it from the component phases.

Synchronous TG/DSC/MS analyses further provided details of the phase transformation and decomposition behaviors of $LiCa(BH_4)_3$. As seen in the DSC profile in Figure 5, the postmilled $LiBH_4/Ca(BH_4)_2$ sample exhibited complicated physical and chemical transformations in the heating process up to 500 °C. Besides the weak signal from the phase transition of $LiBH_4$ at 118 °C, two other mild endothermic peaks were observed at 153 and 203 °C, respectively. Upon heating the sample to over 350 °C, three partially overlapped endothermic peaks appeared, which coincided well with the MS H_2 signals. Apparently, to ascertain the nature of these endothermic events is a central issue in understanding the decomposition behaviors of $LiCa(BH_4)_3$.

In the present study, high temperature phase β-$Ca(BH_4)_2$ was prepared and used as starting material. Furthermore, XRD (Figure 1) and DSC (Figure 2) results well confirmed the phase stability of the individually milled β-$Ca(BH_4)_2$. Therefore, the observed endothermic effect at 153 °C should not be associated with the phase transformation of $Ca(BH_4)_2$,[13] but is an indication of the phase transition of the dual-cation (Li, Ca) borohydride. Here, the similarity of phase transition temperature between the dual-cation borohydride and $Ca(BH_4)_2$ further supports the host/guest roles of $Ca(BH_4)_2/LiBH_4$ in formation of the dual-cation phase. Next, in our effort to ascertain the nature of the endothermic effect at 203 °C, study of the weight fluctuation phenomenon provided a key clue. As shown in Figure 5, the TG profile of the postmilled $LiBH_4/Ca(BH_4)_2$ sample showed acute weight fluctuations in the temperature range 250−360 °C, which were accompanied by the intensity changes of the MS H_2 signal. As a similar phenomenon was also observed in the melting-induced hydrogen release from $LiBH_4$ (Figure 4), we surmised that the weight fluctuation originates from the hydrogen bubbling off the molten $LiCa(BH_4)_3$. To validate this speculation, we heated the sample to different temperatures ranging from 150 to 250 °C and then visually examined the state of the cooled samples. It was found that the postmilled $LiBH_4/Ca(BH_4)_2$ melts around 200 °C. Therefore, the endothermic peak at 203 °C in the DSC profile should be safely ascribed to the melting of $LiCa(BH_4)_3$. In comparison with $LiBH_4$, the dual-cation $LiCa(BH_4)_3$ exhibited more aggravated weight fluctuation. One possible reason is that the molten $LiCa(BH_4)_3$ released much more hydrogen than the molten $LiBH_4$ (~1.2 vs 0.3 wt % H_2). Alternatively, one may argue that the molten $LiCa(BH_4)_3$ reacts with trace amount of $LiBH_4$ or $Ca(BH_4)_2$ residues to form some unstable intermediate phase(s). However, judging from the lack of features of the DSC profile in the temperature range 250−350 °C, the latter possibility seems unlikely.

Notably, the dual-cation $LiCa(BH_4)_3$ differs significantly from the component phases in terms of physical properties ($LiBH_4$ melts around 290 °C; $Ca(BH_4)_2$ undergoes solid phase decomposition without experiencing melting process).[8,13] In the recent

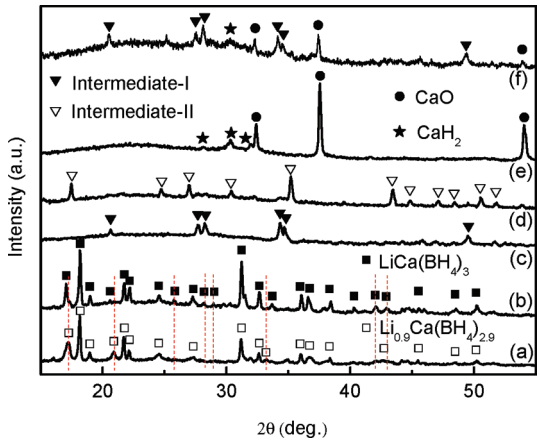

Figure 6. XRD patterns of (a) postmilled $LiBH_4/Ca(BH_4)_2$ and postheated $LiBH_4/Ca(BH_4)_2$ samples at (b) 210, (c) 290, (d) 390, and (e) 450 °C, and (f) rehydrogenated $LiBH_4/Ca(BH_4)_2$ sample at 400 °C.

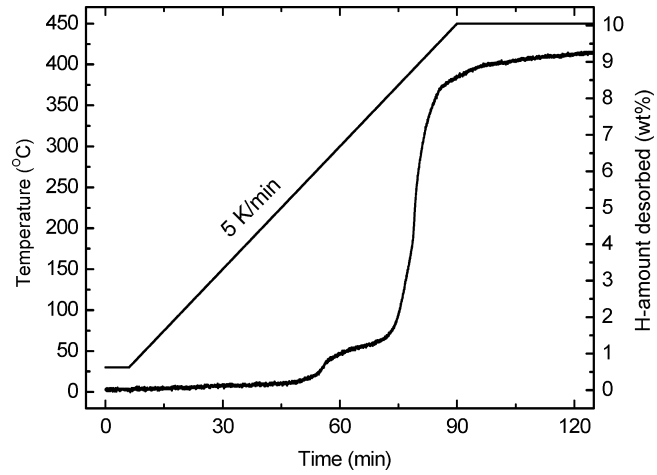

Figure 7. The first dehydrogenation profile of the postmilled $LiBH_4/Ca(BH_4)_2$ sample using TPD method.

study of the series of $xLiBH_4 + (1 - x)Ca(BH_4)_2$ ($x = 0-1$) samples, Lee et al. also observed a similar melting phenomenon, but assigned it to the eutectic melting of $LiBH_4$ and $Ca(BH_4)_2$.[45] As a fundamental basis for such an assignment, Lee et al. claimed that the postmilled sample is a physical mixture of $LiBH_4$ and $Ca(BH_4)_2$. Currently, the reason for this apparent inconsistency is still unclear. One possible reason is that variation of the crystal structure of $Ca(BH_4)_2$ (α- and β-phases of $Ca(BH_4)_2$ were used in the two studies, respectively) results in significantly different reactivity toward $LiBH_4$.

According to the DSC and MS results, the first dehydrogenation step from the molten $LiCa(BH_4)_3$ is a thermoneutral event. By contrast, the subsequent dominant dehydrogenation step was found to be highly endothermic. DSC/MS results showed that the dominant dehydrogenation step of $LiCa(BH_4)_3$ can be further divided into three substages, with the major one peaking at 376 °C and two minor ones at 364 and 402 °C, respectively. Careful examination of the TG/DSC profiles found that the weight fluctuation terminated at the ending stage of the first shoulder peak. This observation indicates that the dominant dehydrogenation process of $LiCa(BH_4)_3$ starts from liquid phase decomposition, as a continuum of the initial H_2 release from the molten sample. The subsequent dehydrogenation proceeds via solid-phase decomposition. According to the MS result, no gas impurity, e.g., diborane (B_2H_6), was detected within the detection limit of the MS apparatus throughout the heating process. The observed weight loss (9.6 wt %) was therefore solely attributed to the hydrogen release, which corresponds to ca. 4.5 H_2 equivalents from $LiCa(BH_4)_3$.

In an effort to follow the phase evolution in the decomposition process of the dual-cation (Li, Ca) borohydride, we carried out ex situ XRD analysis of the samples that were heated to varied temperatures. As shown in Figure 6, the postheated sample at 210 °C exhibited subtle changes in the XRD pattern compared to the postmilled sample, which should be correlated with the transformation of $Li_{0.9}Ca(BH_4)_{2.9}$ into $LiCa(BH_4)_3$. Additionally, it shows clearly the reversibility of the phase transition of $LiCa(BH_4)_3$. In the postheated sample at 290 °C, the diffraction peaks of $LiCa(BH_4)_3$ completely disappeared, and the sample showed a set of new diffraction peaks. Apparently, these new peaks should be assigned to the decomposition product of the first dehydrogenation step, which was temporarily assigned as intermediate phase I. According to the temperature programmed desorption (TPD) result shown below, the first dehydrogenation step released about 1.2 wt % hydrogen, yielding intermediate phase I with a nominal composition of $LiCaB_3H_{11}$. Upon further elevating the pretreatment temperature to 390 °C, the peaks of intermediate phase I disappeared and were replaced by another set of diffraction peaks. This is an indication of the proceeding of the second dehydrogenation step, yielding decomposition product that was assigned as intermediate phase II. Finally, after being heated to 450 °C, the sample showed weak diffraction peaks of CaH_2 and relatively strong peaks of CaO. Here, the identified CaO came from the air contamination of the sample during the XRD measurement. The lack of diffraction peaks of Li- or B-containing phases in the XRD examination indicates their amorphous nature. Similar phenomena were repeatedly observed in the decomposition products of light-metal borohydrides.[8,13,32]

In parallel to the thermal analyses, the dehydrogenation properties of $LiCa(BH_4)_3$ were also examined using a volumetric method. Figure 7 shows the first dehydrogenation profile of the $LiCa(BH_4)_3$ sample using the TPD method. The TPD curve of $LiCa(BH_4)_3$ exhibits a distinct two-step dehydrogenation feature, which agrees reasonably with the thermal analysis results. However, the multistage details of the second dehydrogenation step as observed in the DSC/MS profiles were undistinguishable in the TPD profile. According to the TPD result, the two dehydrogenation steps released 1.2 and 8.1 wt % hydrogen, respectively. The overall dehydrogenation process of $LiCa(BH_4)_3$ can therefore be outlined by eq 2. This is in great contrast to the decomposition behaviors of $LiBH_4$ and $Ca(BH_4)_2$, wherein the generation of intermediate compound containing $[B_{12}H_{12}]^{2-}$ has been proposed as an important dehydrogenation step.[46-51]

$$LiCa(BH_4)_3 \rightarrow LiCaB_3H_{11} + 1/2H_2 \rightarrow LiCa(BH)_3 + 9/2H_2 \quad (2)$$

This finding suggests that the mechanistic decomposition pathway of $LiCa(BH_4)_3$ may differ significantly from that of the constituent borohydrides, which may fundamentally originate from the changes of electronic structure and local coordination of BH_4^- anion in the dual-cation borohydride.

3.3. Re/dehydrogenation in Li−Ca−B−H System. $LiCa(BH_4)_3$ proved a better material for reversible hydrogen storage than its constituent phases. Figure 8 presents the TG profiles of the three samples in the second cycle. In comparison with the single-cation borohydrides, the dual-cation Li−Ca−B−H system showed increased cycling capacity and faster re/dehydrogenation kinetics. According to the MS results (bottom

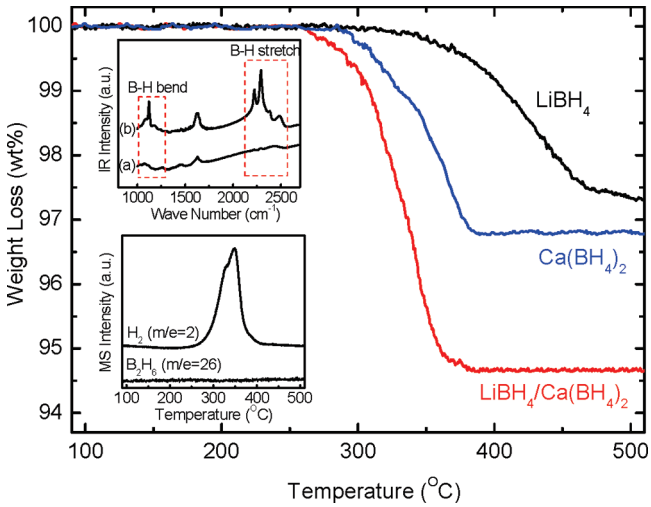

Figure 8. TG profiles of rehydrogenated $LiBH_4$, $Ca(BH_4)_2$, and $LiBH_4/Ca(BH_4)_2$ samples. The upper inset shows the IR spectra of the $LiBH_4/Ca(BH_4)_2$ samples: (a) after dehydrogenation and (b) after rehydrogenation. The bottom inset gives the MS profiles of the rehydrogenated $LiBH_4/Ca(BH_4)_2$ sample.

inset of Figure 8), H_2 is the sole detectable gaseous species from the recharged Li−Ca−B−H sample, which amounts to 5.3 wt % after the sample is heated to 390 °C. Consistently, FTIR analysis of the recharged sample (upper inset of Figure 8) showed clearly the restoration of B−H bands. However, according to the XRD result, the dual-cation $LiCa(BH_4)_3$ cannot be restored under the applied condition. As shown in Figure 6f, the recharged sample showed diffraction peaks of the intermediate phase I that was formed in the first dehydrogenation process of $LiCa(BH_4)_3$, together with weak peaks from residual CaH_2 and CaO contaminant. These results clearly indicate the partial reversibility of the second dehydrogenation step of the Li−Ca−B−H system. In this regard, detailed experimental and theoretical studies are still required to better understand the cyclic dehydrogenation/rehydrogenation behaviors of the Li−Ca−B−H system.

4. Conclusions

Mixed alkali and alkaline-earth metal borohydride, $LiCa(BH_4)_3$, can be readily prepared by mechanically milling 1:1 $LiBH_4/Ca(BH_4)_2$ mixture followed by calcination at elevated temperatures. Compared to the constituent borohydrides, $LiCa(BH_4)_3$ exhibits different physical properties and, particularly, improved de/rehydrogenation properties. For example, a partially reversible dehydrogenation of 5.3 wt % hydrogen had been experimentally elucidated in $LiCa(BH_4)_3$. Additionally, our study showed that the dehydrogenation reaction of $LiCa(BH_4)_3$ may involve a different mechanistic pathway from that of the constituent phases. These findings show the effectiveness of manipulation of multication combination in tuning the hydrogen storage properties of ionic borohydrides. Better mechanistic understanding of the formation and decomposition behaviors of the multication borohydrides may lay an important foundation for the design and synthesis of high-performance borohydrides for reversible hydrogen storage.

Acknowledgment. Financial support from the National Natural Science Foundation of China (50771094 and 50801059), the National Basic Research Program of China (973 Program, 2010CB631305), the Frontier Project of CAS Knowledge Innovation Program (KGCXZ-YW-342), the CAS Special Grant for Postgraduate Research, Innovation, and Practice, KAKENHI (21246100), and the Global-COE Program "Materials Integration (Tohoku University)" is gratefully acknowledged.

References and Notes

(1) Schlapbach, L.; Züttel, A. *Nature* **2001**, *414*, 353.
(2) Schüth, F.; Bogdanović, B.; Felderhoff, M. *Chem. Commun.* **2004**, 2249.
(3) Orimo, S.; Nakamori, Y.; Eliseo, J. R.; Züttel, A.; Jensen, C. M. *Chem. Rev.* **2007**, *107*, 4111.
(4) Züttel, A.; Borgschulte, A.; Orimo, S. *Scr. Mater.* **2007**, *56*, 823.
(5) Vajo, J. J.; Olson, G. L. *Scr. Mater.* **2007**, *56*, 829.
(6) Wang, P.; Kang, X. D. *Dalton Trans.* **2008**, 5400.
(7) Züttel, A.; Rentsch, S.; Fischer, P.; Wenger, P.; Sudan, P.; Mauron, Ph.; Emmenegger, Ch. *J. Alloys Compd.* **2003**, *356*−*357*, 515.
(8) Orimo, S.; Nakamori, Y.; Kitahara, G.; Miwa, K.; Ohba, N.; Towata, S.; Züttel, A. *J. Alloys Compd.* **2005**, *404*−*406*, 427.
(9) Chłopek, K.; Frommen, C.; Léon, A.; Zabara, O.; Fichtner, M. *J. Mater. Chem.* **2007**, *17*, 3496.
(10) Li, H.-W.; Kikuchi, K.; Nakamori, Y.; Ohba, N.; Miwa, K.; Towata, S.; Orimo, S. *Acta Mater.* **2008**, *56*, 1342.
(11) Soloveichik, G. L.; Gao, Y.; Rijssenbeek, J.; Andrus, M.; Kniajanski, S.; Bowman, R. C., Jr.; Hwang, S. J.; Zhao, J. C. *Int. J. Hydrogen Energy* **2009**, *34*, 916.
(12) Miwa, K.; Aoki, M.; Noritake, T.; Ohba, N.; Nakamori, Y.; Towata, S.; Züttel, A.; Orimo, S. *Phys. Rev. B* **2006**, *74*, 155122.
(13) Kim, J.-H.; Jin, S.-A.; Shim, J.-H.; Cho, Y. W. *J. Alloys Compd.* **2008**, *461*, L20.
(14) Majzoub, E. H.; Rönnebro, E. *J. Phys. Chem. C* **2009**, *113*, 3352.
(15) Fichtner, M.; Chlopek, K.; Longhini, M.; Hagemann, H. *J. Phys. Chem. C* **2008**, *112*, 11575.
(16) Kim, Y. Y.; Reed, D.; Lee, Y. S.; Lee, J. Y.; Shim, J.-H.; Book, D.; Cho, Y. W. *J. Phys. Chem. C* **2009**, *113*, 5865.
(17) Vajo, J. J.; Skeith, S. L.; Mertens, F. *J. Phys. Chem. B* **2005**, *109*, 3719.
(18) Bösenberg, U.; Doppiu, S.; Mosegaard, L.; Barkhordarian, G.; Eigen, N.; Borgschulte, A.; Jensen, T. R.; Cerenius, Y.; Gutfleisch, O.; Klassen, T.; Dornheim, M.; Bormann, R. *Acta Mater.* **2007**, *55*, 3951.
(19) Kang, X. D.; Wang, P.; Ma, L. P.; Cheng, H. M. *Appl. Phys. A: Mater. Sci. Process.* **2007**, *89*, 963.
(20) Zhang, Y.; Tian, Q. F.; Zhang, J.; Liu, S. S.; Sun, L. X. *J. Phys. Chem. C* **2009**, *113*, 18424.
(21) Yu, X. B.; Grant, D. M.; Walker, G. S. *J. Phys. Chem. C* **2009**, *113*, 17945.
(22) Yang, J.; Sudik, A.; Wolverton, C. *J. Phys. Chem. C* **2007**, *111*, 19134.
(23) Alapati, S. V.; Johnson, J. K.; Sholl, D. S. *J. Phys. Chem. C* **2008**, *112*, 5258.
(24) Gross, A. F.; Vajo, J. J.; Van Atta, S. L.; Olson, G. L. *J. Phys. Chem. C* **2008**, *112*, 5651.
(25) Fang, Z. Z.; Wang, P.; Rufford, T. E.; Kang, X. D.; Lu, G. Q.; Cheng, H. M. *Acta Mater.* **2008**, *56*, 6257.
(26) Ingleson, M. J.; Barrio, J. P.; Bacsa, J.; Steiner, A.; Darling, G. R.; Jones, J. T. A.; Khimyak, Y. Z.; Rosseinsky, M. J. *Angew. Chem., Int. Ed.* **2009**, *48*, 2012.
(27) Fichtner, M.; Zhao-Karger, Z. R.; Hu, J. J.; Roth, A.; Weidler, P. *Nanotechnology* **2009**, *20*, 204029.
(28) Yin, L. C.; Wang, P.; Fang, Z. Z.; Cheng, H. M. *Chem. Phys. Lett.* **2008**, *450*, 318.
(29) Au, M.; Jurgensen, A. R.; Spencer, W. A.; Anton, D. L.; Pinkerton, F. E.; Hwang, S. J.; Kim, C.; Bowman, R. C., Jr. *J. Phys. Chem. C* **2008**, *112*, 18661.
(30) Fang, Z. Z.; Kang, X. D.; Wang, P.; Cheng, H. M. *J. Phys. Chem. C* **2008**, *112*, 17023.
(31) Li, H.-W.; Kikuchi, K.; Nakamori, Y.; Miwa, K.; Towata, S.; Orimo, S. *Scr. Mater.* **2007**, *57*, 679.
(32) Kim, J.-H.; Shim, J.-H.; Cho, Y. W. *J. Power Sources* **2008**, *181*, 140.
(33) Nakamori, Y.; Miwa, K.; Ninomiya, A.; Li, H.-W.; Ohba, N.; Towata, S.; Züttel, A.; Orimo, S. *Phys. Rev. B* **2006**, *74*, 045126.
(34) Nakamori, Y.; Li, H.-W.; Kikuchi, K.; Aoki, M.; Miwa, K.; Towata, S.; Orimo, S. *J. Alloys Compd.* **2007**, *446*−*447*, 296.
(35) Li, H.-W.; Orimo, S.; Nakamori, Y.; Miwa, K.; Ohba, N.; Towata, S.; Züttel, A. *J. Alloys Compd.* **2007**, *446*−*447*, 315.
(36) Nickels, E. A.; Jones, M. O.; David, W. I. F.; Johnson, S. R.; Lowton, R. L.; Sommariva, M.; Edwards, P. P. *Angew. Chem., Int. Ed.* **2008**, *47*, 2817.
(37) Hagemann, H.; Longhini, M.; Kaminski, J. W.; Wesolowski, T. A.; Černý, R.; Penin, N.; Sørby, M. H.; Hauback, B. C.; Severa, G.; Jensen, C. M. *J. Phys. Chem. A* **2008**, *112*, 7551.

(38) Xiao, X. B.; Yu, W. Y.; Tang, B. Y. *J. Phys.: Condens. Matter* **2008**, *20*, 445210.

(39) Ravnsbæk, D.; Filinchuk, Y.; Cerenius, Y.; Jakobsen, H. J.; Besenbacher, F.; Skibsted, J.; Jensen, T. R. *Angew. Chem., Int. Ed.* **2009**, *48*, 6659.

(40) Choudhury, P.; Srinivasan, S. S.; Bhethanabotla, V. R.; Goswami, Y.; McGrath, K.; Stefanakos, E. K. *Int. J. Hydrogen Energy* **2009**, *34*, 6325.

(41) Seballos, L.; Zhang, J. Z.; Rönnebro, E.; Herberg, J. L.; Majzoub, E. H. *J. Alloys Compd.* **2009**, *476*, 446.

(42) Kim, K. C.; Sholl, D. S. *J. Phys. Chem. C* **2010**, *114*, 678.

(43) Černý, R.; Severa, G.; Ravnsbæk, D. B.; Filinchuk, Y.; D'Anna, V.; Hagemann, H.; Haase, D.; Jensen, C. M.; Jensen, T. R. *J. Phys. Chem. C* **2010**, *114*, 1357.

(44) Fang, Z. Z.; Kang, X. D.; Wang, P.; Li, H. W.; Orimo, S. *J. Alloys Compd.* **2010**, *491*, L1.

(45) Lee, J. Y.; Ravnsbæk, D.; Lee, Y.-S.; Kim, Y.; Cerenius, Y.; Shim, J.-H.; Jensen, T. R.; Hur, N. H.; Cho, Y. W. *J. Phys. Chem. C* **2009**, *113*, 15080.

(46) Orimo, S.; Nakamori, Y.; Ohba, N.; Miwa, K.; Aoki, M.; Towata, S.; Züttel, A. *Appl. Phys. Lett.* **2006**, *89*, 021920.

(47) Ohba, N.; Miwa, K.; Aoki, M.; Noritake, T.; Towata, S.; Nakamori, Y.; Orimo, S.; Züttel, A. *Phys. Rev. B* **2006**, *74*, 075110.

(48) Friedrichs, O.; Remhof, A.; Hwang, S. J.; Züttel, A. *Chem. Mater.* **2010**, *22*, 3265.

(49) Wang, L. L.; Graham, D. D.; Robertson, I. M.; Johnson, D. D. *J. Phys. Chem. C* **2009**, *113*, 20088.

(50) Stavila, V.; Her, J. H.; Zhou, W.; Hwang, S. J.; Kim, C.; Ottley, L. A. M.; Udovic, T. J. *J. Solid State Chem.* **2010**, *183*, 1133.

(51) Ozolins, V.; Majzoub, E. H.; Wolverton, C. *J. Am. Chem. Soc.* **2009**, *131*, 230.

JP109260G